

## Theoretical study of the ideal electrical resistivity of simple fcc metals\*

J. Black<sup>†</sup> and D. L. Mills

*Department of Physics, University of California, Irvine, California 92664*

(Received 2 August 1973)

We have completed a study of the temperature dependence of the ideal electrical resistivity of simple fcc metals, with emphasis on the role of the deviations of the solution of the Boltzmann equation from the simple  $\cos\theta$  form employed frequently in such investigations. We consider a model for which the Fermi surface has spherical shape, but is located near the zone boundaries of an fcc crystal. The temperature dependence of the electrical resistivity has been studied with the use of the variational principle, and a solution constructed from a linear combination of up to nine cubic harmonics. This number is sufficient for the variational calculation to converge over a wide range of temperatures, except at low temperatures ( $\lesssim 10^\circ\text{K}$ ) where the umklapp processes freeze out rapidly. We examine the nature of the solution to the linearized Boltzmann equation and the temperature dependence of the electrical resistivity for three cases: (i) the Fermi surface lies entirely within the first Brillouin zone, with radius appropriate to the belly region of the copper Fermi surface; (ii) the Fermi surface just touches the zone boundary; and (iii) the Fermi surface lies outside the first zone, with radius equal to that of the free-electron sphere appropriate to aluminum.

### I. INTRODUCTION

In simple metals of high purity, the temperature-dependent portion of the electrical resistivity  $\rho$  arises from the scattering of the conduction electrons from phonons. The temperature dependence of  $\rho$  for simple metals has been studied extensively by both theorists and experimentalists for many years. Even though the classic work of Bloch and Grüneisen produced a simple formula for  $\rho$  which exhibits the principal qualitative features observed in many simple metals, many questions may be raised about the assumptions necessary to obtain this result. In fact, a number of issues remain to be completely resolved before a complete theoretical description of the electrical resistance is obtained. The purpose of this paper is to focus attention on one issue which has been addressed by other authors,<sup>1</sup> but which we feel requires further attention.

The calculation of the electron-phonon contribution to  $\rho$  is complicated by two distinct classes of difficulty. First, one must have an accurate description of the Fermi surface of the metal, its phonon spectrum, and the matrix element which controls the electron-phonon scattering. This last quantity requires knowledge of the wave functions of the Bloch electrons near the Fermi surface, and is particularly difficult to compute reliably or to extract from independent data. Furthermore,  $\rho$  is particularly sensitive to this quantity in the region of large wave-vector transfer.

The problems described in the preceding paragraph are all associated with obtaining a realistic quantitative description of the properties of a real metal. Once these difficulties have been overcome in any particular case, one is then faced with the task of extracting the form of the nonequilibrium

portion  $\delta f_{\vec{k}}$  of the electron distribution function from the linearized Boltzmann equation. It appears quite impossible, or at least extremely difficult, to make any progress in solving the linearized Boltzmann equation without resorting to approximations, and the most commonly employed scheme appears hard to justify without further examination. In this approximation the electric field is presumed to displace the Fermi surface rigidly in  $\vec{k}$  space, to produce an electrical current parallel to the field. If the Fermi surface is spherical, then in this scheme,  $\delta f_{\vec{k}}$  is proportional to  $\cos\theta_{\vec{k}}$ , where  $\theta_{\vec{k}}$  is the angle between  $\vec{k}$  and the electric field. One then computes the electrical resistivity by inserting this form of  $\delta f_{\vec{k}}$  into the variational expression for  $\rho$  constructed from the linearized Boltzmann equation.<sup>2</sup>

It is well known that it is difficult to justify this form for  $\delta f_{\vec{k}}$  in temperature regions where  $\rho$  is dominated by the electron-phonon contribution, since even for the simplest metals, the rate of scattering out of a given state  $\vec{k}$  on the Fermi surface increases markedly as the distance between  $\vec{k}$  and the zone boundary decreases. One then expects  $\delta f_{\vec{k}}$  to develop "dimples" centered about those points on the Fermi surface which lie closest to the zone boundary. If one obtains accurate expressions for  $\rho$  through the use of the variational principle and the  $\cos\theta_{\vec{k}}$  form for  $\delta f_{\vec{k}}$ , the reason presumably lies in the variational character of the expression for  $\rho$ , which will allow good values for  $\rho$  to be obtained even for variational expressions for  $\delta f_{\vec{k}}$  which are poor approximations to the true solutions to the linearized Boltzmann equation.

In this paper we present the results of a study of the nature of the solution to the linearized Boltzmann equation for a model of simple fcc metal essentially identical to that employed by Dynes and

Carbotte<sup>3</sup> in aluminum, and more recently by Srivastava<sup>4</sup> in the noble metals.

Our aim is to obtain results for  $\delta f_{\mathbf{k}}$  that are sufficiently accurate for the principal features of the solution to be obtained. We then compute the value and temperature dependence of the electrical resistivity with this solution and compare the results we obtain with those obtained from the  $\cos\theta_{\mathbf{k}}$  ansatz. Thus, for the model, the work serves to outline the regime where the  $\cos\theta_{\mathbf{k}}$  form of  $\delta f_{\mathbf{k}}$  gives reasonable results for  $\rho$  (although we shall see that this form is often a poor approximation to  $\delta f_{\mathbf{k}}$ ).

As we remarked earlier, a number of other authors have also examined this question. Most of this work has confined its attention to the alkali metals (which have the bcc crystal structure) in which the Fermi surface lies farther from the first Brillouin zone than in the fcc structure treated here. As a result, only a small number of variational parameters have been needed to determine the resistivity.<sup>1</sup>

Much of the earlier work also has had as its aim obtaining accurate and realistic results for the resistivity. Our interest is directed also toward the goal of obtaining realistic values of  $\rho$  for real metals, and in addition toward the nature of the form of  $\delta f_{\mathbf{k}}$  that emerges as the solution of the linearized Boltzmann equation, and the variations in this form as the radius of the Fermi surface is changed. Thus, we feel our study is more complete than earlier studies, and the emphasis is also a bit different. We should also mention that some recent calculations<sup>5</sup> employ an analytic approximation scheme to incorporate a boundary condition discussed many years ago by Peierls<sup>6</sup> into the calculation of the low-temperature electrical resistivity of noble metals, where the Fermi surface touches the zone boundary.

The model we employ is the following. We consider a simple metal of the fcc crystal structure. We suppose the Fermi surface is spherical, but both normal and umklapp scattering processes are included in the kernel of the Boltzmann equation. We consider three cases. In case (i), we choose the Fermi surface to lie entirely within the first Brillouin zone, with radius chosen equal to the free electron value appropriate to copper. In case (ii), the Fermi surface is presumed to just touch the zone boundary and in case (iii) the Fermi surface lies outside the first zone with radius equal to that of the free electron sphere appropriate to aluminum.

We construct  $\delta f_{\mathbf{k}}$  by expanding its angular dependence as a linear combination of cubic harmonics. The appropriate linear combination is determined through the use of the variational principle. We have used up to nine cubic harmonics in this expansion,

although we find that the first seven serve to provide rather reasonable forms for  $\delta f_{\mathbf{k}}$ , and addition of the last two change the form of  $\delta f_{\mathbf{k}}$  very little. [One may obtain rather stable and accurate values of  $\rho$  with far fewer variational functions in case (i), as we shall see.]

The outline of this paper is as follows. In Sec. II, we discuss the technical aspects of the calculation common to the three cases. In Sec. III, within three subsections, we present the results for each of the three cases described above. In Sec. IV, we place our results alongside experimental data and other theoretical calculations. When we place our results alongside the data, we must of course keep in mind the oversimplified description of the Fermi surface we use. However, on the basis of our calculations, we do seem able to account for a number of features of the existing data. In Sec. IV, we offer some suggestions why this is so. Finally, in Sec. V we present some concluding remarks.

## II. GENERAL REMARKS

We follow the standard notation,<sup>2</sup> and write the nonequilibrium part of the electron distribution function  $\delta f_{\mathbf{k}}$  in the form

$$\delta f_{\mathbf{k}} = -\frac{\partial f_{\mathbf{k}}^{(0)}}{\partial E_{\mathbf{k}}} \phi(\vec{\mathbf{k}}), \quad (2.1)$$

where  $f_{\mathbf{k}}^{(0)}$  is the equilibrium Fermi-Dirac distribution function and  $E_{\mathbf{k}}$  the energy of an electron with wave vector  $\vec{\mathbf{k}}$ . The electrical resistivity  $\rho$  may be expressed in terms of  $\phi(\vec{\mathbf{k}})$  in the following manner<sup>2</sup>:

$$\rho = P/J^2, \quad (2.2)$$

where for a spherical Fermi surface, and contribution to  $\rho$  from electron-phonon scattering processes we may write  $P$  and  $J$  in the form

$$P = \frac{m^2 k_F^2 \Omega_0}{32\pi^3 \hbar^3 M k_B T} \int \int d\Omega(\hat{n}) d\Omega(\hat{n}') [\phi(\hat{n}) - \phi(\hat{n}')]^2 \times |W(\vec{\mathbf{q}})|^2 \sum_{\lambda} |\vec{\mathbf{q}} \cdot \hat{\mathbf{e}}(\vec{\mathbf{q}}\lambda)|^2 n_{\vec{\mathbf{q}}\lambda} (1 + n_{\vec{\mathbf{q}}\lambda}) \quad (2.3a)$$

and

$$J = \frac{ek_F^2}{4\pi^3 \hbar} \int d\Omega(\hat{n}) (\hat{n} \cdot \hat{\mathbf{z}}) \phi(\hat{n}). \quad (2.3b)$$

In the above expressions,  $M$  is ionic mass,  $\Omega_0$  is the volume per ion,  $m$  is the band-structure effective mass of the conduction electron (we use the free-electron mass in calculations unless otherwise indicated),  $\vec{\mathbf{q}} = k_F(\hat{n} - \hat{n}')$  is the wave-vector transfer suffered by the electron in an electron-phonon collision, and  $|W(\vec{\mathbf{q}})|^2$  is the square of the pseudopotential form factor which, following earlier authors,<sup>1</sup> we presume depends only on the magnitude of the wave-vector transfer. Also  $\hat{\mathbf{e}}(\vec{\mathbf{q}}\lambda)$  is the

polarization vector of the phonon responsible for the scattering, and  $n_{\vec{q}}$  the Bose-Einstein occupation number of the phonon. In Eq. (2.3a), the contribution from both  $N$  processes and  $U$  processes is included. The wave vector  $\vec{q}$  is the change in wave vector suffered by the electron in the electron-phonon collision. If  $\vec{q}$  lies within the first Brillouin zone, it is equal to the wave vector  $\vec{Q}$  of the phonon which produces the scattering, and it is equal to  $\vec{Q} + \vec{G}$  if it lies outside, where  $\vec{G}$  is a reciprocal-lattice vector. The periodic character in momentum space of the dynamical matrix which generates the phonon frequencies and eigenvectors insures that the eigenvectors and frequencies evaluated at the wave vector  $\vec{Q} + \vec{G}$  are identical to those at  $\vec{Q}$ . We ignore phonon drag effects here, so the phonons remain in thermal equilibrium. In Eq. (2.3b),  $\hat{z}$  is a unit vector in the direction of the applied electric field, presumed to be parallel to the  $\hat{z}$  axis. Following the standard procedure to derive these results,  $\phi(\vec{k})$  along with other quantities that vary slowly with  $|\vec{k}|$  have been evaluated on the Fermi surface, so  $\vec{k} = k_F \hat{n}$ , where  $\hat{n}$  is a unit vector.

The result in Eq. (2.2) forms a variational expression for the electrical resistivity.<sup>2</sup> Therefore, our procedure will be to expand  $\phi(\hat{n})$  in terms of an orthogonal set of functions  $\{\phi_i(\hat{n})\}$ ,

$$\phi(\hat{n}) = \sum_{i=1}^N \eta_i \phi_i(\hat{n}) \quad (2.4)$$

and we shall determine the coefficients  $\eta_i$  by minimizing the resistivity functional in Eq. (2.2). Then for  $P$  we have the form

$$P = \sum_{ij} \eta_i \eta_j P_{ij}, \quad (2.5a)$$

and for  $J$ , we have

$$J = \sum_i \eta_i J_i. \quad (2.5b)$$

Then if  $P_{ij}^{-1}$  denotes the  $ij$ th element of the  $N \times N$  matrix, that is, the inverse of  $P_{ij}$ , for  $\eta_i$ , we have<sup>2</sup>

$$\eta_i = \sum_j P_{ij}^{-1} J_j E_0,$$

where  $E_0$  is the electric field strength.

We have chosen the functions  $\phi_i(\hat{n})$  to be the first nine cubic harmonics that are odd under reflection in the  $xy$  plane, normal to the  $\hat{z}$  axis, and which have the azimuthal symmetry appropriate to the fourfold rotation symmetry of the fcc Brillouin zone about the  $\hat{z}$  axis. These functions are listed in Table I.

The quantities  $P_{ij}$  were evaluated by direct numerical computation of the fourfold integration of the expression deduced from Eq. (2.3a). The program constructed for this purpose employed Simpson's rule, and a CDC 7600 was used for the calculations. For our purposes, we found direct

evaluation of the four-dimensional integrals more convenient than schemes which reduce the four-dimensional integral to a three-dimensional one, such as that discussed by Ekin and Bringer.<sup>1</sup>

The integrations were performed using the variables  $\mu (= \cos\theta)$  and  $\phi$ , where  $\theta$  and  $\phi$  are the usual spherical coordinates. In this scheme an element of solid angle becomes

$$d\Omega = -d\mu d\phi, \quad (2.6)$$

and equal solid angle elements may be used by making equal increments in  $\mu$  and  $\phi$ . The finest meshes employed are shown in Table II. For meshes  $A$  and  $B$  the scattering was taken from initial states on  $\frac{1}{18}$ th of the Fermi surface to final states which range over the whole Fermi surface, and thus the mesh only partly exploits the cubic symmetry. In meshes  $C$  and  $D$  the cubic symmetry was exploited fully by using only  $\frac{1}{48}$ th of the Fermi surface for initial states, and computing  $[\phi(\hat{n}) - \phi(\hat{n}')]^2$  for the three scattering events which are equally probable due to the cubic symmetry. Mesh  $E$  proved useful in the evaluation of the normal part of the resistivity at low temperatures, where the final states lie close in angle on the Fermi surface to the initial states because only small scattering vectors contribute to the resistivity.

### III. DISCUSSION OF RESULTS

In this section, we describe the results of the resistivity calculations carried out by the methods described in Sec. II. As we mentioned in Sec. I, we have examined three distinct cases. In the first, the Fermi surface lies entirely within the first Brillouin zone; in the second, it just touches the zone boundary; and in the third, it lies entirely outside the first Brillouin zone. We discuss the results for each case in separate subsections.

TABLE I. Tabulation of the nine cubic harmonics employed in the calculation of the electrical resistivity in the present work.

$i$	$(\mu = \cos\theta)$ $\phi_i(\hat{n})$
1	$\mu$
2	$\frac{5}{2}(\mu^3 - \frac{3}{2}\mu)$
3	$\frac{1}{6}(63\mu^5 - 70\mu^3 + 15\mu)$
4	$945\mu(1 - \mu^2)^2 \cos 4\phi$
5	$\frac{1}{16}(429\mu^7 - 693\mu^5 + 315\mu^3 - 35\mu)$
6	$\frac{5465}{2}(1 - \mu^2)^2(13\mu^3 - 3\mu) \cos 4\phi$
7	$\frac{1}{128}(12155\mu^9 - 25740\mu^7 + 18018\mu^5 - 4620\mu^3 + 315\mu)$
8	$16891.875(1 - \mu^2)^2(17\mu^5 - 10\mu^3 + \mu) \cos 4\phi$
9	$34459425(1 - \mu^2)^4 \mu \cos 8\phi$

TABLE II. Various meshes used in the numerical integration routines.

Mesh size	$\theta$ (deg)			$\phi$ (deg)			$\theta^1$ (deg)			$\phi^1$ (deg)		
	Initial	Final	No. of steps	Initial	Final	No. of steps	Initial	Final	No. of steps	Initial	Final	No. of steps
A	0	90	9	0	45	5	0	180	17	0	360	25
B	0	90	9	0	45	7	0	180	17	0	360	49
C	0	54.73	9	0 <sup>a</sup>	45	7	0	180	17	0	360	49
D	0	54.73	9	0 <sup>a</sup>	45	7	0	35	5	0	360	25
							35	75	9	0	360	49
							75	105	5	0	360	25
							105	145	9	0	360	49
E	0	90	21	0	45	3	0	14	11	0	360	25
							14	30	11	0	360	25

<sup>a</sup>For  $\theta > 45^\circ$  the limits on the initial value of  $\phi$  vary to give exactly  $\frac{1}{48}$ th of the first Brillouin zone.

(i) Case where the Fermi surface lies entirely within the first Brillouin zone

While our simple model cannot be presumed to provide a complete description of the electrical resistivity of the noble metals because of its oversimplified treatment of the Fermi surface, nonetheless we shall use data appropriate to copper in this first study. In the calculations, we have employed the pseudopotential form factor of Moriarty.<sup>7</sup> We shall also take the radius of the Fermi surface to be that of a monovalent fcc metal. In units of  $2\pi/a$ , then  $k_F = 0.7816$ . In the [111] direction, the distance from the origin of  $\vec{k}$  space to the face of the Brillouin zone is 0.8660, in these same units. This is the direction where the Fermi surface comes closest to the zone boundary.

Force constants of Nicklow *et al.*<sup>8</sup> were used in a Born-Von Karmon calculation to determine the phonon eigenvectors and eigenfrequencies as described by Dynes and Carbotte.<sup>3</sup> Separate sets of force constants were determined by these authors for  $T = 49^\circ\text{K}$ , and  $T = 298^\circ\text{K}$ . The former set has been employed in our (constant volume) resistivity calculations from 0 to  $175^\circ\text{K}$ , and the latter set from  $175$  to  $1360^\circ\text{K}$ , the melting temperature of copper. We note in passing that Svenson *et al.*<sup>9</sup> have also determined a set of force constants at  $296^\circ\text{K}$  for copper. At  $298^\circ\text{K}$ , these force constants give for  $\rho$  a value of the resistivity (calculated with only one term in  $\phi(\hat{n})$ ) only 1.6% higher than the value calculated by a similar method from the force constants of Nicklow *et al.*

The results of a series of resistivity calculations that employ from one to nine terms in the ex-

pansion displayed in Eq. (2.4) are presented in Table III. We note that with the possible exception of the  $10^\circ\text{K}$  case, all the calculated resistivities have converged to three significant figures by the time nine terms have been included in the calculation. Even at  $10^\circ\text{K}$ , the result has very nearly converged.

There are some striking features in these results. If we presume that our calculation has converged to the exact resistivity of our model metal throughout the range of temperatures displayed in Table III, then for all temperatures greater than  $80^\circ\text{K}$ , we obtain the correct value of  $\rho$  to within 5% if only the first term (the "cos $\theta$ " term) is retained in the calculation. However, the number of terms required increases significantly as the temperature is lowered below this value. By the time  $T = 49^\circ\text{K}$ , four terms are required, and at least six by the time  $T = 10^\circ\text{K}$ . We also note that inclusion of the second, fourth, and sixth terms influence the resistivity dramatically.

We should remark that while the sequence of resistivity values tabulated in Table III for a given value of the temperature converges to three figure accuracy, as described in the preceding paragraph, one must realize that the mesh utilized in each calculation may not have been sufficiently fine to insure that each integral had in fact been computed to the full three-figure accuracy. Thus, the numbers in Table III associated with a given temperature provide a comparison between successive values of the resistivity computed for the particular mesh indicated in the far-right column, as the number of cubic harmonics in the expansion of

TABLE III. Electrical resistivity ( $\mu\Omega$  cm) as a function of temperature, and of the number of terms included in the expansion of  $\phi(\hat{n})$  for the case where the Fermi surface lies within the first Brillouin zone.

Temp. (°K)	Multiply table value by	Number of terms in the expansion of $\phi(\hat{n})$									Mesh size
		1	2	3	4	5	6	7	8	9	
1365	$10^1$	1.88	1.88	1.88	1.86	1.86	1.85	1.85	1.85	1.85	A
900	$10^1$	1.24	1.23	1.23	1.22	1.22	1.21	1.21	1.21	1.21	A
600	$10^0$	8.20	8.13	8.13	8.06	8.06	8.00	8.00	8.00	8.00	A
400	$10^0$	5.38	5.35	5.35	5.29	5.29	5.26	5.26	5.26	5.26	A
298	$10^0$	3.91	3.89	3.89	3.85	3.85	3.83	3.83	3.83	3.83	B
175	$10^0$	2.09	2.07	2.07	2.05	2.05	2.04	2.04	2.04	2.04	B
175 <sup>a</sup>	$10^0$	1.85	1.84	1.84	1.82	1.81	1.81	1.81	1.81	1.81	B
80	$10^{-1}$	5.26	5.18	5.18	5.05	5.05	4.96	4.96	4.96	4.96	B
49	$10^{-1}$	1.55	1.49	1.48	1.38	1.38	1.33	1.33	1.33	1.33	B
30	$10^{-2}$	2.68	2.37	2.35	1.91	1.90	1.74	1.72	1.69	1.68	C
20	$10^{-3}$	3.69	2.44	2.34	1.63	1.61	1.42	1.42	1.38	1.36	C
10	$10^{-6}$	46.2	8.02	6.82	4.86	4.78	4.49	4.49	4.36	4.34	D

<sup>a</sup>Force constants obtained at 49°K used for this and lower temperatures. Force constants obtained at 298°K used above this entry.

$\phi(\hat{n})$  is increased. We feel that the numbers in Table III have converged to within 1% of the actual value of the resistivity of the model for temperatures above 175°K, and this deteriorates to about 5% at 10°K. We did not extend the calculations below 10°K because we felt that even with our finest mesh (mesh D), the convergence became poor rapidly below 10°K, to the point where the calculations could not be regarded as reliable. We did not have the resources to pursue the behavior of the resistivity in the low-temperature region.

We now turn to the second phase of this study in which we wish to study the form of  $\phi(\hat{n})$ , as a function of temperature. As we see from Table III, by the time six terms have been included in the expansion of  $\phi(\hat{n})$ , the resistivity has converged to within

5% of its final value even at the lowest temperatures. This fact, when combined with considerations of the mesh size we have employed, suggests that we restrict our study of  $\phi(\hat{n})$  to results obtained with six terms in the expansion.<sup>10</sup> The coefficients of the six terms, normalized so the coefficient of the first term is unity, are presented in Table IV. [Of course, when  $\rho$  is computed from Eq. (3.2),  $\phi(\hat{n})$  may be multiplied by an arbitrary value without affecting the value of  $\rho$ .]

In studies of the effects of mesh size we find that the second, fourth, and sixth coefficients have converged to  $\approx 15\%$  of their final value. The third and fifth coefficients are considerably worse, but this originates because they contribute relatively little to the resistivity, as can be seen from

TABLE IV. Coefficients  $\{\eta_i\}$  which appear in the expansion of  $\phi(\hat{n})$  for the case where the Fermi surface lies within the first Brillouin zone. The coefficients are normalized so that  $\eta_1$  is unity.

Temp. (°K)	Index of the coefficient						Mesh size
	1	2	3	4	5	6	
Multiplying factor	$10^0$	$10^{-2}$	$10^{-2}$	$10^{-4}$	$10^{-2}$	$10^{-5}$	
1365	1.00	7.95	1.69	4.33	-1.33	8.45	A
900	1.00	7.99	1.70	4.35	-1.33	8.49	A
600	1.00	8.04	1.71	4.37	-1.33	8.55	A
400	1.00	8.17	1.72	4.45	-1.32	8.71	A
298	1.00	8.33	1.68	4.51	-1.29	8.81	B
175	1.00	9.12	1.79	4.96	-1.27	9.77	B
175	1.00	8.63	1.38	4.77	-1.15	9.60	B
80	1.00	12.5	1.63	7.17	-0.996	15.4	B
49	1.00	17.7	0.732	11.1	-0.353	25.9	B
30	1.00	15.0	-14.4	16.5	-2.90	41.3	C
20	1.00	17.6	-13.8	18.1	-8.82	41.7	C
10	1.00	65.9	31.7	11.1	-8.96	13.5	D

Table III.

We note that above 175 °K, the set of coefficients  $\{\eta_i\}$  change little with temperature. This is expected when one is well above the Debye temperature, since then the Bose-Einstein functions in the expression for  $\rho$  may be replaced by their high-temperature limiting form, and the temperature drops out of the integrals.

It is not easy to jump from the table of coefficients to a physical picture of the effects on  $\phi(\hat{n})$  of adding additional terms. To gain insight into what is involved, we have plotted on a stereographic projection a function we have called  $R(\hat{n})$ . The function  $R(\hat{n})$  is defined by

$$R(\hat{n}) = \phi(\hat{n})/\eta_1 \cos\theta. \quad (3.1)$$

The function  $R(\hat{n})$  is equal to unity for all values of  $\hat{n}$ , if  $\phi(\hat{n})$  is well approximated by the  $\cos\theta$  form of the solution. We can expect  $R(\hat{n})$  to fall below unity on those portions of the Fermi surface where the electrons are scattered most strongly by the phonons. This should occur on those portions of the Fermi surface which lie closest to the Brillouin-zone boundary, since at these points, the umklapp processes are strong throughout the temperature range explored here.

We should say a few more words about the physical significance of  $R(\hat{n})$ . Since the functions  $\phi_i(\hat{n})$  included in the expansion of  $\phi(\hat{n})$  [Eq. (2.4)] are mutually orthogonal, and the function  $\cos\theta$  is among the set, the quantity  $J^2$  which appears in Eq. (2.3b) is simply a constant multiplied by  $\eta_1^2$ . As a consequence, we can rewrite the expression for  $\rho$  in a form with only the numerator  $P$  present, but with

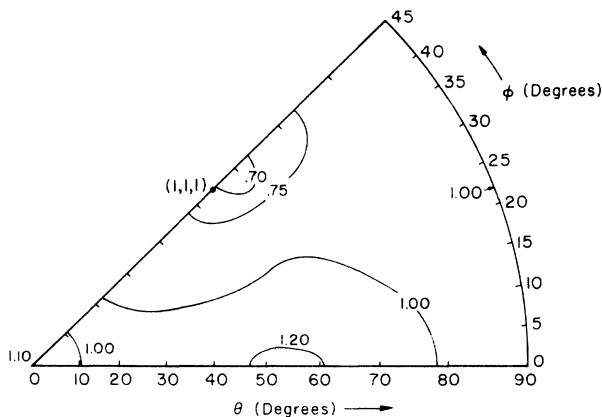


FIG. 1. Stereographic projection of the function  $R(\hat{n})$  defined in Eq. (3.1) for  $T=298^\circ\text{K}$ , where  $\phi(\hat{n})$  is given by the six-term approximation. The electric field is applied along the  $\hat{z}$  axis ( $\theta=0$ ), and the point of closest approach of the Fermi surface to the zone boundary occurs when  $\theta = \cos^{-1}(1/\sqrt{3}) = 54.7^\circ$  and  $\phi = 45^\circ$ . The Fermi surface is inside the first Brillouin zone.

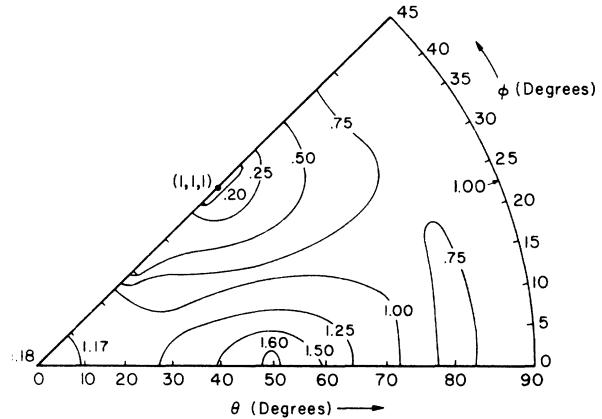


FIG. 2. Stereographic projection constructed as in Fig. 1 for  $T=49^\circ\text{K}$ .

$[\phi(\hat{n}) - \phi(\hat{n}')]^2$  replaced by the combination  $[\phi(\hat{n})/\eta_1 - \phi(\hat{n}')/\eta_1]^2$ . If only one term is present in the expansion, this reduces to  $(\cos\theta - \cos\theta')^2$ , but in the general case it becomes  $[R(\hat{n})\cos\theta - R(\hat{n}')\cos\theta']^2$ . Thus, the function  $R(\hat{n})$  provides one with a convenient measure of the manner in which departures from the  $\cos\theta$  form of  $\phi(\hat{n})$  affect the resistivity.

For a sequence of four temperatures, we present the stereographic projections in Figs. 1–4. In these figures, the electric field is applied along the direction  $\theta=0$ , parallel to the  $[001]$  axis of the crystal. The point of closest approach of the Fermi surface to the zone boundary is along the  $[111]$  direction, and this point is located along the line  $\phi=45^\circ$ , at  $\theta = \cos^{-1}(1/\sqrt{3}) \approx 55^\circ$ . The point  $\phi=45^\circ$  and  $\theta=90^\circ$  is the  $[110]$  direction, and  $\phi=0^\circ$ ,  $\theta=90^\circ$  is the  $[100]$  direction.

From Fig. 1, one can see that while there are well defined and clear deviations of  $\phi(\hat{n})$  from the  $\cos\theta$  form of the solution, these deviations are not dramatic in character. There is a dip in  $\phi(\hat{n})$  centered about the point  $\phi=45^\circ$ ,  $\theta = \cos^{-1}(1/\sqrt{3})$ , where the scattering rate is particularly large because of the umklapp processes. The function  $\phi(\hat{n})$  has a broad maximum along the line  $\phi=0^\circ$ , which sweeps from the  $[001]$  to the  $[100]$  direction as  $\theta$  sweeps from  $0^\circ$  to  $90^\circ$ .

By the time the temperature drops to  $49^\circ\text{K}$  (Fig. 2), we see that the angular variation of  $\phi(\hat{n})$  becomes very pronounced. The dip centered around the  $[111]$  direction is now a very strong one, and at the minimum, which is quite broad in its angular range,  $\phi(\hat{n})$  assumes a value only 20% of that expected if the  $\cos\theta$  form is used. At the same time, the maximum along the direction  $\phi=0^\circ$  is much more prominent than it was at the higher temperatures. Even though we see from Fig. 2 that  $\phi(\hat{n})$  is poorly approximated by the  $\cos\theta$  form at  $T$

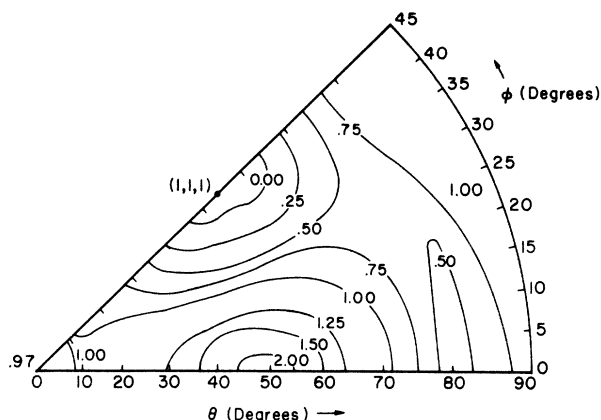


FIG. 3. Stereographic projection constructed as in Fig. 1 for  $T=30^\circ\text{K}$ .

$=49^\circ\text{K}$ , the resistivity computed from the  $\cos\theta$  form differs from the best value computed from the full form of  $\phi(\hat{n})$  by only about 15%, as one can see from Table III. This is presumably because of the variational character of the expression for the resistivity in Eq. (2.2).

From Fig. 3 and Fig. 4, one can see that the minimum at 10 and  $30^\circ\text{K}$  becomes extremely pronounced. Indeed, our calculation produces negative values for  $\phi(\hat{n})$  in these regions. We feel that these negative values are unphysical, and result from the fact that we retain only a finite number of terms in our expression for  $\phi(\hat{n})$ . When the dip in  $\phi(\hat{n})$  becomes very sharp and extends only over a relatively small angular range, quite clearly many terms in the cubic harmonic expansion must be included before an accurate description of  $\phi(\hat{n})$  may be obtained. A proper and accurate description of  $\phi(\hat{n})$  in the small angular region near the bottom of the dip may also require the use of a finer mesh so the coefficients  $\eta_i$  may be evaluated more accurately. We feel that the values of  $\rho$  we compute are not affected greatly by the behavior of our approximate form for  $\phi(\hat{n})$  in the immediate region of the dip, since  $\phi(\hat{n})$  is negative only over a small angular range, and its absolute value is very small compared to its value elsewhere.

We have seen from the above analysis that  $\phi(\hat{n})$  has a strong minimum in the  $z$  direction where the Fermi surface comes closest to the zone boundary, particularly at low temperatures. This is, of course, where the umklapp scattering rate is largest. Thus, if one decomposes the resistivity into a portion  $\rho_N$  that arises from only  $N$  processes, and a portion  $\rho_U$  which comes only from  $U$  processes, one expects  $\rho_U$  to be strongly affected by the dip in  $\phi(\hat{n})$ , while  $\rho_N$  should be less sensitive to this feature. We have explored this point by recalculating the resistivity assuming only  $N$  pro-

cesses are operative (and  $U$  processes are inoperative). We find that  $\rho_N$  is quite insensitive to the number of terms included in  $\phi(\hat{n})$ , except at the very lowest temperatures. At  $1^\circ\text{K}$  there was a nine per cent reduction in the value of  $\rho$  computed when six terms are included, and the result is compared with that obtained with the  $\cos\theta$  form of  $\phi(\hat{n})$ .

(ii) Case where the Fermi surface touches the zone boundary

In these calculations, we have used the same integration procedures and model parameters as in case (i), where the Fermi surface was assumed to lie entirely within the zone boundary. The only difference here is that we allow the radius of the Fermi surface to expand until the Fermi surface just touches the  $\langle 111 \rangle$  face of the Brillouin zone. Of course, the Fermi sphere just touches all the Brillouin-zone faces in the  $[111]$  direction, and since these faces lie closest to the origin of  $\vec{k}$  space, in the  $[100]$  direction where the distance from the origin to the zone face is  $2\pi/a$ , the Fermi surface lies within the first zone.

The results for the temperature dependence and magnitude of the electrical resistivity are given in Table V. Once again, the calculations have employed up to nine terms in the expansion of  $\phi(\hat{n})$ . We note that convergence to three figures has occurred by the time nine terms are included for temperatures down to  $49^\circ\text{K}$ , but below this temperature a significant lowering of the resistivity occurs as we go from eight to nine terms. In the temperature range from 175 to  $1356^\circ\text{K}$ , inclusion of only four terms in  $\phi(\hat{n})$  brings the resistivity to within 5% of the final value computed with nine terms; by the time  $80^\circ\text{K}$  is reached five terms are required, and six by the time the temperature drops to  $49^\circ\text{K}$ . Below this temperature eight or more terms are needed, and we cannot be certain

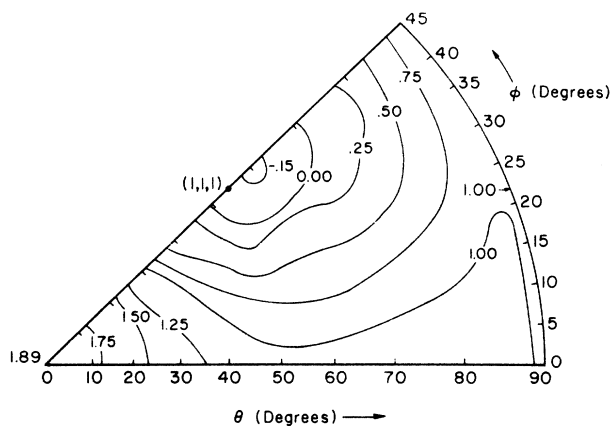


FIG. 4. Stereographic projection constructed as in Fig. 1 for  $T=10^\circ\text{K}$ .

TABLE V. Resistivity (in  $\mu\Omega$  cm) for the case where the Fermi surface just touches the Brillouin-zone boundary, as a function of the number of terms in  $\phi(\hat{n})$ .

Temp. (°K)	Multiply table value by	Number of terms in expansion of $\phi(\hat{n})$									Mesh size
		1	2	3	4	5	6	7	8	9	
1356	$10^1$	3.42	3.09	3.08	2.58	2.52	2.44	2.44	2.44	2.44	A
900	$10^1$	2.27	2.04	2.04	1.70	1.67	1.62	1.62	1.61	1.61	A
600	$10^1$	1.51	1.35	1.35	1.13	1.10	1.07	1.07	1.07	1.07	A
298	$10^0$	7.19	6.49	6.49	5.46	5.32	5.15	5.15	5.15	5.15	A
175	$10^0$	4.10	3.60	3.60	2.94	2.87	2.78	2.78	2.77	2.77	A
175	$10^0$	3.47	3.12	3.12	2.61	2.54	2.46	2.46	2.46	2.45	B
80	$10^0$	1.25	1.03	1.03	0.794	0.769	0.735	0.735	0.735	0.730	B
49	$10^{-1}$	5.15	3.92	3.92	2.64	2.51	2.35	2.35	2.31	2.30	C
30	$10^{-1}$	2.08	1.04	1.04	0.571	0.526	0.481	0.472	0.431	0.417	C
20	$10^{-2}$	9.71	2.27	2.24	1.23	1.12	1.06	0.925	0.699	0.649	C
10	$10^{-4}$	279.	8.16	4.01	3.46	2.73	2.73	2.58	1.58	1.32	D

our calculation has converged without including more than nine terms.

In case (i) we saw that use of the  $\cos\theta$  form produced rather accurate values of the resistivity at high temperatures  $T > \Theta_D$  even though our study of the form of  $\phi(\hat{n})$  indicated that  $\phi(\hat{n})$  showed significant deviations from the  $\cos\theta$  form. In contrast to the former case, approximation of  $\phi(\hat{n})$  by the  $\cos\theta$  form produces values of the resistivity higher than the final values by roughly 30%.

We have tested the convergence of the numerical calculations by comparing some values of the resistivity listed in Table V with values computed with different meshes. The results of this investigation are discussed in Appendix A and may be summarized as follows. For the case where only one term is present in  $\phi(\hat{n})$  [ $\phi(\hat{n})$  has the  $\cos\theta$  form], use of a finer mesh shows the resistivity values in Table V should be reduced by perhaps 8% in the temperature region from 80 to 1356 °K.

These results have been obtained by repeating the calculations with mesh C instead of mesh A. The relatively poor convergence found when the  $\cos\theta$  form of  $\phi(\hat{n})$  is used with mesh A presumably has its origin in the singularity present in the integral along the [111] direction where the Fermi surface touches the zone boundary, and very small wave vector phonons lead to umklapp scattering. With two or more terms present in  $\phi(\hat{n})$ , the meshes employed to generate the numbers in Table V give results accurate to roughly 1% for  $T \geq 298$  °K, and to roughly 5% by 49 °K.

In Table VI we present the coefficients obtained for the case where six terms are included in  $\phi(\hat{n})$ . Note that once again, in the region  $T \geq 175$  °K, the coefficients change little with temperature. The most accurate set of coefficients are those computed with mesh C at 298 °K; one may presume  $\phi(\hat{n})$  is accurately represented by these values in the high temperature region. The coefficient  $\eta_3$

TABLE VI. Coefficients  $\{\eta_i\}$  in the expansion of  $\phi(\hat{n})$ , for the case where the Fermi surface just touches the zone boundary in the [111] direction.

Temp. (°K)	Index of the coefficient						Mesh size
	1	2	3	4	5	6	
Multiplying factor	$10^0$	$10^{-1}$	$10^{-2}$	$10^{-3}$	$10^{-1}$	$10^{-4}$	
1356	1.00	1.58	-1.28	1.18	-2.27	2.12	A
900	1.00	1.58	-1.31	1.18	-2.28	2.13	A
600	1.00	1.58	-1.39	1.18	-2.28	2.13	A
298	1.00	1.65	-1.44	1.20	-2.40	2.20	B
298	1.00	1.28	-5.40	1.22	-2.65	2.04	C
175	1.00	1.58	-2.87	1.23	-2.34	2.25	A
175	1.00	1.62	-2.62	1.23	-2.41	2.29	B
80	1.00	1.56	-8.88	1.40	-2.60	2.77	B
49	1.00	0.744	-25.6	1.67	-3.28	3.41	C
30	1.00	0.550	-36.7	1.80	-3.25	3.80	C
20	1.00	1.57	-22.0	1.73	-2.81	3.01	C
10	1.00	1.30	+105.0	0.554	4.26	0.025	D

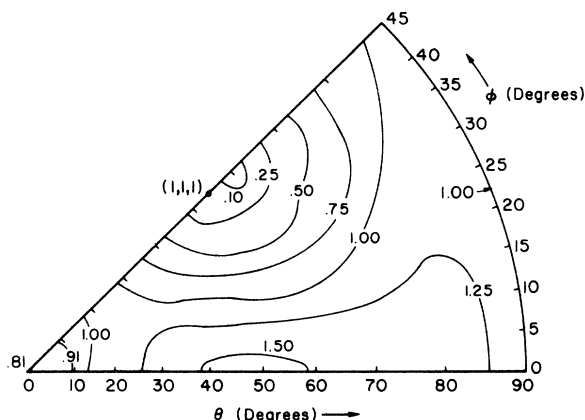


FIG. 5. Stereographic projection of the function  $R(\hat{n})$  for  $T=298^\circ\text{K}$ , where  $\phi(\hat{n})$  is given by the six-term approximation and the Fermi surface just touches the first Brillouin zone in the  $[111]$  direction.

varies in a somewhat erratic manner. We find this term in the expansion of  $\phi(\hat{n})$  contributes little to the electrical resistivity, except at the low end of the temperature range. For  $T \leq 49^\circ\text{K}$  we believe the second, fourth, fifth, and sixth coefficients are accurate to within  $\approx 10\%$ . In Appendix A we have illustrated and discussed the convergence.

In Figs. 5–8, we present again the stereographic projections of the function  $R(\hat{n})$  defined in Eq. (3.1). Several remarks are in order about these results.

First, it is apparent that we always find a very sharp dip in  $\phi(\hat{n})$  in the  $[111]$  direction for this case, even at elevated temperatures, as illustrated in Fig. 5. Recall that in case (i), at elevated temperatures, while  $\phi(n)$  dipped quite noticeably in the  $[111]$  direction (see Fig. 1),  $\phi(\hat{n})$  did not deviate from the  $\cos\theta$  value by more than 30%. The solution displayed in Fig. 5 shows that at its minimum

value,  $R(\hat{n})$  dips to roughly 0.05, which means that in the  $[111]$  direction  $\phi(\hat{n})$  assumes the value of 0.03, compared to the value of  $\approx 0.6$  expected for the  $\cos\theta$  form of the solution.

We have here a direct test of the accuracy of our scheme for generating values of  $\phi(\hat{n})$ . The reason is that one may argue quite generally that at points where the Fermi surface touches the zone boundary, one must have  $\phi(\hat{n})$  identically equal to zero. This follows because, to phrase the argument in language appropriate to the present geometry, if we consider any one particular point  $\hat{n}_1$  on the zone boundary, there is one other point  $\hat{n}_2$  on the zone boundary in the opposite  $[111]$  direction removed from  $\hat{n}_1$  by precisely a reciprocal lattice vector of the crystal. Thus  $\hat{n}_1$  and  $\hat{n}_2$  refer to exactly the same electron state, and we must have  $\phi(\hat{n}_1) = \phi(\hat{n}_2)$  as a consequence. But the inhomogeneous driving term in the linearized Boltzmann equation is an odd function of  $\cos\theta$ ; from this it follows that  $\phi(\hat{n})$  must be an odd function of  $\cos\theta$ . Thus, we conclude  $\phi(\hat{n}_1) = -\phi(\hat{n}_2)$ . The only way to satisfy these two conditions simultaneously is to have  $\phi(\hat{n}_1) = \phi(\hat{n}_2) = 0$ , and one concludes that  $\phi(\hat{n})$  must vanish identically at each of the points in the  $[111]$  direction where the Fermi surface of our model touches the zone boundary. This argument was discussed in detail many years ago by Peierls,<sup>6</sup> and it has also formed the basis in the recent literature for analytic schemes<sup>5</sup> that may be used to study the behavior of the electrical resistivity at very low temperatures, when the Fermi surface touches the zone boundary.

Thus, if our scheme produced the exact values of  $\phi(\hat{n})$ , we should find for this case that  $\phi(\hat{n})$  assumes its minimum value precisely in the  $[111]$  direction, and that the minimum value of  $\phi(\hat{n})$  is identically zero. If one examines the data in Figs. 5–8, one sees that  $\phi(\hat{n})$  assumes a value quite close

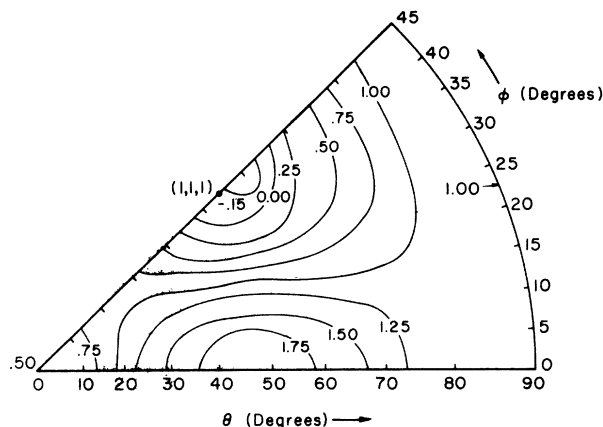


FIG. 6. Stereographic projection constructed as in Fig. 5 for  $T=49^\circ\text{K}$ .

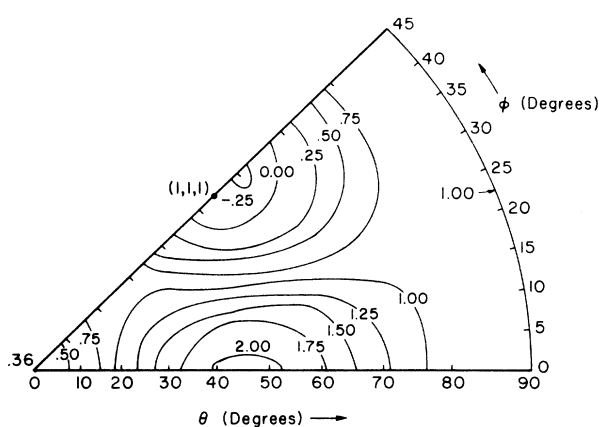


FIG. 7. Stereographic projection constructed as in Fig. 5 for  $T=30^\circ\text{K}$ .

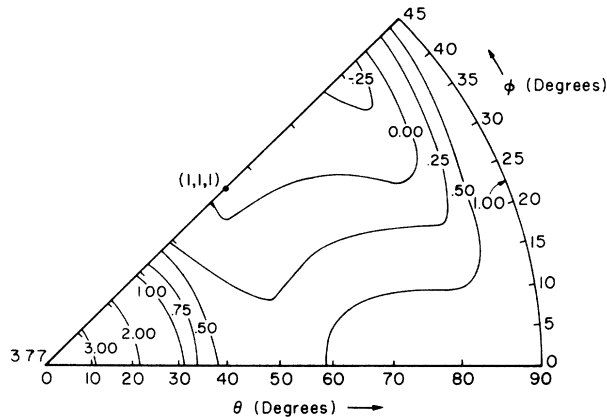


FIG. 8. Stereographic projection constructed as in Fig. 5 for  $T=10^\circ\text{K}$ .

to zero, but not identically equal to zero, in the  $[111]$  direction. At  $298^\circ\text{K}$  (Fig. 5), we find a minimum value of  $\approx 0.03$  removed from the  $[111]$  direction by a few degrees. At  $T=49^\circ\text{K}$ , and  $T=30^\circ\text{K}$ ,  $\phi(\hat{n})$  again has a zero very near the  $[111]$  direction, although the negative values of  $\phi(\hat{n})$  in the small angular region near  $\theta=60^\circ$  and  $40^\circ < \phi < 45^\circ$  may have their origin in the fact that we are approximating a function which contains a rather sharp dip in it by a finite number of terms. At  $T=10^\circ\text{K}$ , these negative values extend over a wider range of  $\theta$ , and the comparatively slow convergence of the values of  $\phi(\hat{n})$  will be required to give an accurate result for both  $\rho$ , and for  $\phi(\hat{n})$ .

In summary, we feel that the approximate form we obtain for  $\phi(\hat{n})$  reproduces the expected behavior with good accuracy over a wide range of temperature. Even at high temperatures, we see  $\phi(\hat{n})$  dip sharply to near zero in the  $[111]$  direction, as the Peierls boundary condition requires; this behavior was absent in case (i). Our results appear quite reasonable except at the lowest temperatures. The dip evidently becomes sharper and more pronounced as the temperature is lowered (one expects this because the umklapp processes begin to freeze out most rapidly for points removed from the  $[111]$  direction), and there is a point where our expansion in no more than nine cubic harmonics becomes inadequate. By the time  $T=30^\circ\text{K}$ , our form for  $\phi(\hat{n})$  exhibits a "ringing" behavior over a small solid angle region and overshoots the zero. By the time  $T=10^\circ\text{K}$ , the values produced for  $\phi(\hat{n})$  raise some question in our minds, and this is reinforced by the very slow convergence of  $\rho$  as additional terms are added to  $\phi(\hat{n})$ .

It should also be noticed that in the  $[001]$  direction (parallel to the external field), the Fermi surface lies quite close to the zone boundary. The

umklapp scattering processes are quite strong here also, and one should expect  $\phi(\hat{n})$  to exhibit a minimum here also. One sees this minimum as a very well defined feature in Figs. 5–7. It becomes particularly sharp at  $T=49^\circ\text{K}$ , and  $T=30^\circ\text{K}$ . At these temperatures, the umklapp scattering rate is large at the  $(0, 0, 1)$  point on the Fermi surface, but "freezes out" rather rapidly as one moves down the Fermi surface by increasing the azimuthal angle  $\theta$ . One then obtains the pronounced minimum in  $\phi(\hat{n})$  displayed in Figs. 6 and 7. At  $10^\circ\text{K}$  these processes appear to have frozen out of the resistivity, and the dip feature in  $\phi(\hat{n})$  has been replaced with a rise.

(iii) Case where the Fermi surface lies outside the first Brillouin zone

In this subsection we apply the methods used in the two preceding subsections to the analysis of the behavior of the electrical resistivity and the distribution function  $\phi(\hat{n})$  for the case where the Fermi surface lies outside the first Brillouin zone. Just as we chose the input parameters for the model to mimic the properties of copper as closely as possible, for the present case we choose the parameters to be characteristic of aluminum. Since aluminum is a trivalent metal, the radius of the free electron Fermi surface appropriate to aluminum is  $1.1272$ , in units of  $2\pi/a$ . This should be compared with the distance from the origin of  $\vec{k}$  space and the point farthest from the origin on the surface of the first Brillouin zone. This point lies at the intersection of a  $(100)$  plane and the line between two touching  $(111)$  planes; the distance of this point from the zone center is  $1.1180$  units.

To carry out the electrical resistivity calculations, we have used the Heine–Abarenkov form factors as tabulated by Harrison,<sup>11</sup> and the phonon force constants of Gilat and Nicklow<sup>12</sup> obtained at  $80^\circ\text{K}$ .

The results of the resistivity calculations are presented in Table VII. We note that down to  $40^\circ\text{K}$ , the use of seven terms in  $\phi(\hat{n})$  produces convergence to three figures, but below this, and in particular at  $10^\circ\text{K}$ , there is a clear need for additional terms in the expansion. Note that if we presume the resistivity for the model is accurately given by the nine-term form for  $\phi(\hat{n})$ , then convergence to within 5% of the correct value has occurred with four terms for  $T \geq 195^\circ\text{K}$ , five terms for  $T=80^\circ\text{K}$ , seven terms for  $T=40^\circ\text{K}$ , and eight terms for  $T=25^\circ\text{K}$ .

The accuracy associated with the meshes employed in the resistivity calculation is as follows. For the  $\cos\theta$  form of  $\phi(\hat{n})$  (only one term in the expansion), the results are accurate to 5% for  $T \geq 195^\circ\text{K}$ . The accuracy deteriorates as the temperature is lowered until, for  $T=30^\circ\text{K}$ , the result

TABLE VII. Resistivity (in  $\mu\Omega$  cm) for the case where the Fermi surface lies just outside the Brillouin-zone boundary, as a function of the number of terms in  $\phi(\hat{n})$ .

Temp. (°K)	Multiply table value by	Number of terms in expansion of $\phi(\hat{n})$									Mesh size
		1	2	3	4	5	6	7	8	9	
934	$10^0$	6.58	6.37	6.37	6.37	6.25	6.21	6.06	6.06	6.06	C
660	$10^0$	4.61	4.48	4.48	4.48	4.37	4.37	4.25	4.25	4.25	C
390	$10^0$	2.66	2.58	2.58	2.58	2.51	2.51	2.44	2.44	2.44	C
195	$10^0$	1.20	1.15	1.15	1.15	1.11	1.11	1.08	1.08	1.08	C
80	$10^{-1}$	2.99	2.68	2.67	2.65	2.44	2.44	2.33	2.33	2.33	C
40	$10^{-2}$	5.24	3.65	3.65	3.37	2.86	2.78	2.57	2.55	2.54	D
25	$10^{-3}$	15.7	7.25	7.04	4.85	3.40	3.26	3.05	2.65	2.57	D
10	$10^{-4}$	14.9	3.99	3.30	1.35	0.748	0.738	0.708	0.388	0.317	D

for the  $\cos\theta$  solution may be off by 30%, and by  $10^\circ\text{K}$  as much as a factor of 3. As additional terms are added to  $\phi(\hat{n})$ , the numerical integration scheme becomes more accurate so that for the seven-term solution, our tests show the numerical results accurate to 1% for  $T \geq 195^\circ\text{K}$ , 5% for  $T = 40^\circ\text{K}$ , and 10% for  $T = 10^\circ\text{K}$ .

In Table VIII, we have presented the coefficients obtained for the seven-term expansion of  $\phi(\hat{n})$ . Note that the third and the sixth terms contribute little to changes in the resistivity until we reach  $10^\circ\text{K}$ , at which point these coefficients change dramatically. An investigation of the convergence of these coefficients as far as the mesh size is concerned shows that all coefficients have converged to within 25% of their correct value, and many have converged far more accurately than that.

The function  $R(\hat{n})$  is plotted in Figs. 9–11. The dashed lines on the figures indicate the locus of closest approach of the Fermi surface and the Brillouin zone. (These are lines of intersection of the Brillouin-zone boundary faces.) Particularly at the two lowest temperatures, one can see a pronounced depression of  $\phi(\hat{n})$  near these lines. Presumably it is the large depressed areas then that

give rise to the reduction in resistivity as we go from one to seven terms in the expansion of  $\phi(\hat{n})$ .

#### IV. COMPARISON BETWEEN THEORY AND EXPERIMENT

The purpose of this section is to compare the results of the calculations described in Sec. III with some experimental data on systems that may be approximately described by our models.

While the calculations described above were carried out with the use of realistic phonon spectra and pseudopotential form factors which are believed qualitatively and very likely quantitatively accurate, we have made one major approximation by replacing the true Fermi surface by the free-electron spheres appropriate to the cases examined in Sec. III. We begin this section by presenting the results of some calculations which suggest that this approximation does not lead to serious quantitative errors.

Consider case (i), where the Fermi sphere lies entirely within the first Brillouin zone, but comes quite close to its boundaries in the [111] direction. It is well known that in copper, the Fermi surface develops necks which extend out to and touch the zone boundaries in the [111] direction. Quite

TABLE VIII. Coefficients  $\{\eta_i\}$  in the expansion of  $\phi(\hat{n})$ , for the case where the Fermi surface lies just outside the zone boundary.

Temp. (°K)	Coefficient index							Mesh size
	1	2	3	4	5	6	7	
Multiplying factor	$10^0$	$10^0$	$10^{-1}$	$10^{-3}$	$10^0$	$10^{-4}$	$10^0$	
934	1.00	-0.246	-0.594	-0.145	0.204	-0.528	0.367	C
660	1.00	-0.248	-0.597	-0.147	0.205	-0.530	0.366	C
390	1.00	-0.257	-0.617	-0.156	0.212	-0.543	0.372	C
195	1.00	-0.290	-0.700	-0.195	0.242	-0.600	0.394	C
80	1.00	-0.478	-1.11	-0.499	0.434	-0.963	0.514	C
40	1.00	-0.694	-1.91	-1.61	0.765	-2.20	0.656	D
25	1.00	-0.881	-1.40	-2.62	1.02	-2.08	0.493	D
10	1.00	-0.834	+1.74	-3.20	1.13	+0.526	0.318	D



TABLE IX. Effect of  $14^\circ$  caps on the value of the resistivity ( $\mu\Omega$  cm), for the case where the Fermi surface lies inside the zone boundary.

Temp. (°K)	Multiply table value by	Caps removed	Number of terms									Mesh size
			1	2	3	4	5	6	7	8	9	
298	$10^0$	Yes	3.77	3.76	3.76	3.75	3.75	3.73	3.73	3.73	3.73	<i>B</i>
	$10^0$	No	3.90	3.89	3.89	3.85	3.85	3.83	3.83	3.83	3.83	<i>B</i>
49	$10^{-1}$	Yes	1.36	1.35	1.35	1.30	1.30	1.26	1.26	1.26	1.26	<i>B</i>
	$10^{-1}$	No	1.55	1.49	1.48	1.38	1.38	1.33	1.33	1.33	1.33	<i>B</i>
10	$10^{-6}$	Yes	13.5	3.69	2.97	2.44	2.35	2.31	2.27	2.26	2.26	<i>B</i>
	$10^{-6}$	No	44.2	5.69	3.36	2.85	2.65	2.60	2.54	2.54	2.53	<i>B</i>

the Fermi surface which are close to the zone boundaries.

It must be emphasized that our conclusion that the details of the scattering kernel near the  $[111]$  direction are relatively unimportant rests strongly on the fact that  $\phi(\hat{n})$  is determined solely or predominantly by the electron-phonon scattering rate. If the contribution to  $\rho$  from impurity scattering is greater than, or perhaps comparable to, that from electron-phonon scattering, then  $\phi(\hat{n})$  will be more closely approximated by the  $\cos\theta$  form, and the resistivity at low temperatures will be sensitive to the manner in which the Fermi surface and electron-phonon matrix element are described in the neck region of the Fermi surface.

Next we turn to a comparison of our results for case (i) with the experimental data for copper. Consider first the region  $T \geq 175^\circ\text{K}$ , where the resistivity throughout this range is computed with phonon force constants determined at  $298^\circ\text{K}$ . We find that  $\rho$  increases linearly with temperature; between  $400$  and  $135^\circ\text{K}$ , our results are fit by a straight line to better than 1%, and the same line lies 8% above the value of  $\rho$  at  $175^\circ\text{K}$ . These results are not surprising in view of the fact that the Debye temperature  $\Theta_D$  of copper is  $320^\circ\text{K}$ .

At  $295^\circ\text{K}$ , our calculated resistivity is larger by a factor of 2.2 than the value given for copper in Ref. 13. At  $1356^\circ\text{K}$ , our calculated resistivity, after correcting it to atmospheric pressure, is 2.1 times the value quoted by Cussak<sup>14</sup> for this temperature. In this temperature range, recall that there is little difference between the values of  $\rho$  computed from the one term or the nine term expression for  $\phi(\hat{n})$ .

Srivastava<sup>4</sup> has carried out resistivity calculations for copper in the temperature range  $15^\circ\text{K} < T < 300^\circ\text{K}$ . He used only the  $\cos\theta$  form in the expansion of  $\phi(\hat{n})$ , along with the form factors of Moriarty,<sup>7</sup> as we have done. At  $300^\circ\text{K}$ , his results are in good accord with ours, but they differ considerably as the temperature is lowered, and by  $20^\circ\text{K}$  his results are larger than those we obtain when we use the  $\cos\theta$  form of  $\phi(\hat{n})$  by a factor of

20. While we cannot pin down the precise reasons for this discrepancy, as we have tried to emphasize in the discussions in Sec. III, one must exercise considerable care in the low-temperature regime to insure that the numerical integrations are accurate. We are led to question his use of the spherical six term integration procedure due to Houston.<sup>15</sup> Also, he has described the phonon spectrum through the use of a simple phonon spectrum developed by Krebs,<sup>16</sup> and this may lead to further quantitative discrepancies between his results and ours.

In Fig. 12, we have plotted the results of our calculations of the resistivity for the one-, two-, and six-term expansion of  $\phi(\hat{n})$ . The quantity is plotted in the ratio  $\rho/T^5$ . Note the growth of pronounced differences between the results computed with different numbers of terms in  $\phi(\hat{n})$  as the temperature is lowered. The dashed lines in the figure are sketched in to indicate the approximate behavior of  $\rho/T^5$  below  $10^\circ\text{K}$ , a region we did not explore in detail. At  $1^\circ\text{K}$ , where the umklapp processes have frozen out to a very good approximation, we did perform a calculation of the normal resistivity which employed mesh *E*. The results of this calculation are represented by a single point, since there is little difference between the results obtained with the different forms of  $\phi(\hat{n})$ .

We should remark that Ekin and Bringer<sup>1</sup> have explored the effect of modifying the  $\cos\theta$  form of  $\phi(\hat{n})$  on the electrical resistivity of potassium. They obtained the largest departures from the  $\cos\theta$  solution when they included terms equivalent to our first three terms in the expansion of  $\phi(\hat{n})$ . They found that a maximum change of 12% in the computed values of  $\rho$  resulted when their result was compared to that obtained from the  $\cos\theta$  form of  $\phi(\hat{n})$ . This occurred at  $T = 5^\circ\text{K}$ . Primarily because of the increased proximity of the Fermi surface to the zone boundary in the fcc structure, the effects of using more than one term in the expansion of  $\phi(\hat{n})$  are more dramatic in our model of copper.

In Fig. 12 we have superimposed several sets of

experimental data, namely, the data of Schriempf,<sup>17</sup> White and Woods,<sup>18</sup> and the very recent data of Rumbo.<sup>19</sup> Schriempf studied three samples, and we have reproduced data from his purest sample.

White and Woods<sup>18</sup> were able to fit their data in the temperature range from 10 to 30 °K with a  $T^{5.1}$  law. We note that our calculations show that the temperature is not yet sufficiently low for this to be interpreted as the low-temperature limiting behavior of the resistivity expected on the basis of, for example, the Bloch-Grüneisen law. In the temperature region between 10 and 30 °K, the plot of  $\rho/T^5$  shows this function to have a broad maximum. At low temperatures, the umklapps freeze out rapidly, so  $\rho$  varies more rapidly than  $T^5$ , and at higher temperatures,  $\rho$  varies more slowly than  $T^5$  simply because  $kT/\Theta_D$  is large enough for significant deviations from the low-temperature behavior to occur.

In Fig. 12 the maximum in our calculated values of  $\rho/T^5$  with the six-term form of  $\phi(\hat{n})$  is considerably sharper than the maximum observed by White and Woods. It must be kept in mind that in the calculations presented here, we have assumed that only electron-phonon scattering is present. Actually, as the temperature is lowered, one passes from a regime where the phonon scattering dominates the impurity scattering, to the low-temperature regime where the converse is true. At temperatures where impurity scattering is strong compared to phonon scattering, one expects  $\phi(\hat{n})$  to be

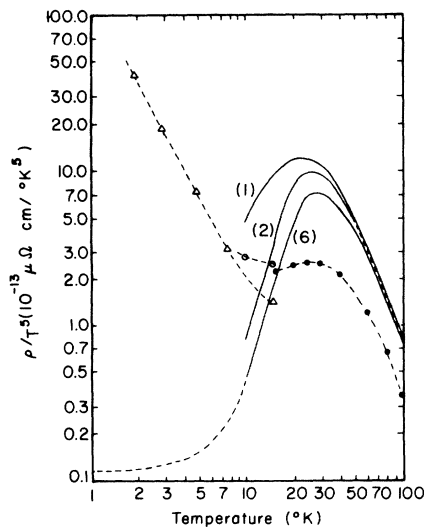


FIG. 12. Calculated resistivity divided by temperature to the fifth power vs temperature. The Fermi surface lies inside the first Brillouin zone. Experimental data shown for copper are due to  $\Delta$ , Rumbo (Ref. 18);  $\circ$ , Schriempf (Ref. 16); and  $\bullet$ , White and Woods (Ref. 17). The quantity in brackets is the number of terms in the expansion of  $\phi(\hat{n})$ .

closely approximated by the  $\cos\theta$  form, since it is known that  $\phi(\hat{n})$  has precisely this form<sup>2</sup> in the presence of only impurity scattering when the Fermi surface is spherical. Thus, crudely speaking, as the temperature is lowered, one expects  $\phi(\hat{n})$  to gradually shift over from the full form we use to the  $\cos\theta$  form. (The importance of this effect was first pointed out by Kagan and Zhernov.<sup>1</sup>) Upon comparing the curve for  $\rho/T^5$  computed with the six-term expression for  $\phi(\hat{n})$  with that computed from the  $\cos\theta$  form, one can see that the transition from the phonon scattering dominated regime to the impurity scattering dominated region should broaden the maximum in  $\rho/T^5$ , if this transition occurs near 30 °K in copper. From the data of White and Woods, we estimate that at 40 °K, their sample is indeed in the regime where electron-phonon scattering makes the dominant contribution to  $\rho$ , while at  $T=15$  °K, the temperature dependent portion of  $\rho$  is a small fraction of the total, so one is well into the regime where impurity scattering dominates.

The data of Schriempf appears qualitatively consistent with the results of our calculations, although the resistivities measured by him appear considerably larger than the results obtained by White and Woods.

The recent low-temperature data of Rumbo are particularly striking, since the measurements were made on copper of high purity, and the data show dramatic deviations of a qualitative kind from the results we obtain. Rumbo points out that his data are well fitted by an empirical relation which presumes the resistivity to vary as  $T^3$ . It seems highly unlikely that we could reproduce these data with any modification of the form factors, or other ingredients of our model. Thus, the present work is unable to shed light on the origin of this striking behavior. We do note that a  $T^3$  variation of the resistivity at low temperatures has been observed in many metals,<sup>20</sup> and a simple empirical rule appears to account for its magnitude. Also, Ehrlich<sup>5</sup> has discussed a means of producing a  $T^2$  term in  $\rho$  at low temperatures in the presence of both impurity and electron-phonon scattering and necks on the Fermi surface. Wilkins and Lawrence have also discussed the possibility that a  $T^2$  term may occur in  $\rho$  at low temperatures. We are not aware, however, of any theoretical mechanism which produces a  $T^3$  term.

In summary, in the temperature range from 15 °K up to the melting temperature, our calculations produce values of the electrical resistivity for copper which lie between two and four times the values measured experimentally. This sort of error is quite respectable since we have not adjusted the form factors in any way to fit the data. The accuracy we obtain is comparable to that ob-

tained in recent studies of the alkali metals.

We next examine some of the results obtained for case (ii), where the Fermi surface was presumed to just touch the boundary of the first Brillouin zone.

In the high-temperature region ( $T \geq 175^\circ\text{K}$ ), we find a linear dependence of the resistivity on temperature. Now, however, unlike the situation in case (i), the value of  $\rho$  is sensitive to the number of terms in the expansion of  $\phi(\hat{n})$ . Note also that the value of  $\rho$  at a given temperature is considerably larger for case (ii) than for case (i). Also, we now require a number of terms in the expansion of  $\phi(\hat{n})$  to obtain an accurate value of  $\rho$ , where as remarked above, in the results presented for case (i), the  $\cos\theta$  form of  $\phi(\hat{n})$  gave accurate values of  $\rho$  in the high-temperature region.

The effect on the resistivity of introducing  $14^\circ$  caps is presented in Table X for the three temperatures  $T=10$ , 49, and  $298^\circ\text{K}$ . The results are rather similar to those for case (i) in that by the time the full nine-term expression for  $\phi(\hat{n})$  is used, so  $\phi(\hat{n})$  is small near the (111) faces of the Brillouin zone, the resistivity is rather insensitive to modifications of the kernel of the Boltzmann equation in this region of the Fermi surface. At high temperatures ( $T=298^\circ\text{K}$ ), the resistivity changes by a considerable amount, the order of 30%, when the caps are removed. Recall from the discussion for case (i) that at  $298^\circ\text{K}$  we found only an 8% reduction in resistivity when the cap scattering was removed.

There is no elemental material at high temperatures with which we can compare these calculations. However, we can apply the calculations to describe the resistivity of those copper based substitutional binary alloys which have an electron/atom ratio larger than pure copper, if we presume that the effect of alloying may be represented simply by increasing the radius of the Fermi sphere so that the Fermi surface contains the proper number of electrons for the alloys. Within this model, as the concentration of the dilute constituent is increased, the radius of the Fermi surface increases until it touches the Brillouin-zone boundary.

If this model is a reasonable first approximation to a description of the alloy, then one should expect the value of the lattice resistivity observed in the high-temperature region to depend only on the electron/atom ratio. Upon comparing the value of  $\rho$  at a given temperature we obtain for case (ii) with that obtained in case (i), we also expect  $\rho$  at a given temperature to increase monotonically as electrons are added.

A complete set of data on the electrical resistivity of alloys of copper with zinc, gallium, germanium, and arsenic and its dependence on composition has been reported by Crisp, Henry, and Schroeder.<sup>21</sup> From their data, we have plotted the lattice resistivity as a function of the radius of the appropriate free-electron sphere, and while we do find that there is some structure in the plot, particularly on the dilute end for those elements which lie farthest from copper in the Periodic Table, all the data indeed tend to cluster about the same straight line. To compute the radius of the Fermi sphere, we have assumed that addition of zinc adds one electron/zinc atom to the conduction band, addition of gallium adds two, and so on. Thus, the data follow the trends we expect from our calculations; namely, the lattice resistivity at a given temperature increases monotonically as the radius of the free-electron Fermi sphere increases, and the rate of increase of  $\rho$  depends primarily on the electron-to-atom ratio.

Unfortunately, the data do not involve alloys sufficiently concentrated for the Fermi surface to touch the zone boundary. Thus, for  $T=298^\circ\text{K}$ , we have recalculated the resistivity for selected Fermi radii inside the zone, for values of the Fermi wave vector larger than that of copper. The results are displayed in Table XI, along with data on the lattice resistivity of the copper-zinc system at  $T=290^\circ\text{K}$  taken from the paper of Crisp *et al.*,<sup>21</sup> since the lattice resistivity may be determined most accurately from their data for this system. The calculations surely reproduce the trends evident in the data. To make the comparison explicit, from the data one has

TABLE X. Effects of  $14^\circ$  caps on the value of the resistivity ( $\mu\Omega\text{ cm}$ ), for the case where the Fermi surface just touches the zone boundary.

Temp. ( $^\circ\text{K}$ )	Multiply table value by	Caps removed	Number of terms in expansion of $\phi(\hat{n})$									Mesh size
			1	2	3	4	5	6	7	8	9	
298	$10^0$	Yes	5.26	5.24	5.21	5.00	4.95	4.85	4.85	4.85	4.85	<i>B</i>
	$10^0$	No	7.19	6.49	6.49	5.46	5.32	5.15	5.15	5.15	5.15	<i>B</i>
49	$10^{-1}$	Yes	3.51	3.29	3.27	2.46	2.33	2.15	2.14	2.14	2.13	<i>C</i>
	$10^{-1}$	No	5.15	3.92	3.92	2.64	2.51	2.35	2.35	2.31	2.30	<i>C</i>
10	$10^{-4}$	Yes	8.16	4.46	3.36	2.30	2.27	2.27	2.06	1.34	1.01	<i>C</i>
	$10^{-4}$	No	27.9	8.16	4.01	3.46	2.73	2.73	2.58	1.58	1.32	<i>D</i>

TABLE XI. Effects on resistivity ( $\mu\Omega$  cm) of varying the size of the Fermi radius. (Mesh C used in all cases).

Radius of Fermi surface ( $2\pi/a$ )	Measured value <sup>a</sup>	Number of terms in the expansion of $\phi(\hat{n})$								
		1	2	3	4	5	6	7	8	9
0.7816	1.64	3.92	3.91	3.91	3.86	3.86	3.85	3.79	3.78	3.78
0.8027	1.89	4.31	4.27	4.27	4.18	4.18	4.17	4.10	4.10	4.10
0.8238	2.15	4.78	4.74	4.74	4.57	4.55	4.50	4.44	4.44	4.44
0.8430	2.44	5.40	5.29	5.29	4.95	4.90	4.83	4.76	4.76	4.76
0.8660	...	6.85	6.41	6.41	5.49	5.38	5.24	5.18	5.18	5.18

<sup>a</sup>Obtained at 290 °K using Cu-Zn.

$$\frac{\rho(0.7816)}{\rho(0.8430)} \Big|_{\text{expt}} = 0.675, \quad (4.1a)$$

while from the calculations

$$\frac{\rho(0.7816)}{\rho(0.8430)} \Big|_{\text{TH}} = 0.79. \quad (4.1b)$$

The calculations clearly produce the trends evident in the data, with good semiquantitative agreement on the order of magnitude of the variation of  $d\rho/dT$ .

Some additional comments on the manner in which the experimental numbers in Table XI were determined are in order. We have used the copper-zinc<sup>21</sup> data of Crisp *et al.*, because it is the most accurate in the region of interest. The numbers in Table XI were obtained by interpolation between the actual experimental points. In order to compare experiment with theory, one must proceed with some care. For pure copper, the value of  $\rho$  of 3.78  $\mu\Omega$  cm is indeed the correct value for our model, at  $T=298$  °K. As the radius of the Fermi sphere is increased by alloying, of course this is done by increasing the zinc concentration, the residual resistivity of the alloy necessarily increases. By the time the Fermi wave vector  $k_F$  is 0.8430 in our dimensionless units, the residual resistivity and the lattice resistivity are close to each other in magnitude. This means that when  $k_F=0.8430$ , it is misleading to use our nine term form of  $\phi(\hat{n})$ , with the coefficients determined from only the electron-phonon scattering, to compute the resistivity of the alloy. The presence of the impurity scattering tends to "drive" the form of  $\phi(\hat{n})$  toward the  $\cos\theta$  form since in our model this is the form  $\phi(\hat{n})$  will assume if only impurity scattering is present. If we make the extreme assumption that  $\phi(\hat{n})$  is given by the  $\cos\theta$  form when  $k_F=0.8430$ , but by the full nine-term form for pure copper, the theoretical value of the ratio displayed in Eq. (4.1b) becomes

$$\frac{\rho(0.7816)}{\rho(0.8430)} = \frac{3.78}{5.40} = 0.70, \quad (4.1c)$$

a value remarkably close to the observed ratio displayed in Eq. (4.1a). Thus, we suspect that if we determined the form of  $\phi(\hat{n})$  by allowing the form of  $\phi(\hat{n})$  to be influenced by the presence of the strong impurity scattering present in the concentrated alloy, our model could provide a rather quantitative account of the alloy data. The result displayed in Eq. (4.1c) is encouraging, and we are pursuing this point further. [Of course, when the form of  $\phi(\hat{n})$  is influenced by both impurity and electron-phonon scattering, then it is no longer possible to separate  $\rho$  into two additive terms, one which represents only the impurity scattering, and one which represents only the lattice contribution, i. e., Mathiessen's rule will then not be applicable. However, when the impurity scattering is so strong that  $\phi(\hat{n}) \approx \cos\theta$  at all temperatures of interest, this separation is again possible, and this is what we assume for  $k_F=0.8430$  when the ratio in Eq. (4.1c) is formed. For this value of  $k_F$ , Mathiessen's rule is still not applicable in the strict sense, of course, since the lattice contribution to  $\rho$  assumes a value significantly different from that in pure Cu.]

A plot of the ratio  $\rho/T^5$  for case (ii), where the Fermi surface just touches the zone boundary, is presented in Fig. 13. We have replotted for comparison purposes the results of the calculation for case (i), where the  $\cos\theta$  form of  $\phi(\hat{n})$  has been used. The chief difference between the results for case (i) and case (ii) are that in the latter case, there is no onset of the "freezing out" phenomena even by 10 °K, when the  $\cos\theta$  form of  $\phi(\hat{n})$  is used for case (ii). The value of  $\rho/T^5$  continues to rise monotonically as  $T$  decreases, well below the temperature of the turnover for  $\rho/T^5$  when the  $\cos\theta$  form of  $\phi(\hat{n})$  is used for case (i). However, by the time nine terms are used in the expansion of  $\phi(\hat{n})$ , the plot of  $\rho/T^5$  for case (ii) assumes a form rather similar in its qualitative features to the curves for case (i).

Ekin and Bringer<sup>1</sup> explored the effect of expanding the Fermi surface of potassium on  $\phi(\hat{n})$  resistivity. They found the greatest differences between resistivities computed with one and more terms in

$\phi(\hat{n})$  to occur when the Fermi surface touched the zone boundary. At that Fermi radius they found the largest effects at  $T = 1^\circ\text{K}$  (their calculations do not go below this temperature) where the one term and many term resistivities differed by a factor of about 2.

We have not attempted to compare the results of our calculations with data at low temperatures. This would require explicit inclusion of both impurity and electron-phonon scattering before a reasonable comparison could be made. Also, since our experiment to prove the sensitivity of  $\rho$  to removal of the caps near the (1, 1, 1) point of the Brillouin zone indicates that at low temperatures, when the  $\cos\theta$  form of  $\phi(\hat{n})$  is used, the value obtained for  $\rho$  becomes very sensitive to the manner in which those regions of the Fermi surface which lie close to the zone boundary are treated. Thus, the problem of computing realistic values of  $\rho$  at low temperatures for even a very simple model of the alloy becomes quite a complex task which we have not addressed.

Finally, in this section, we explore the results obtained in Sec. III for case (iii), where the Fermi surface lies entirely outside the first Brillouin

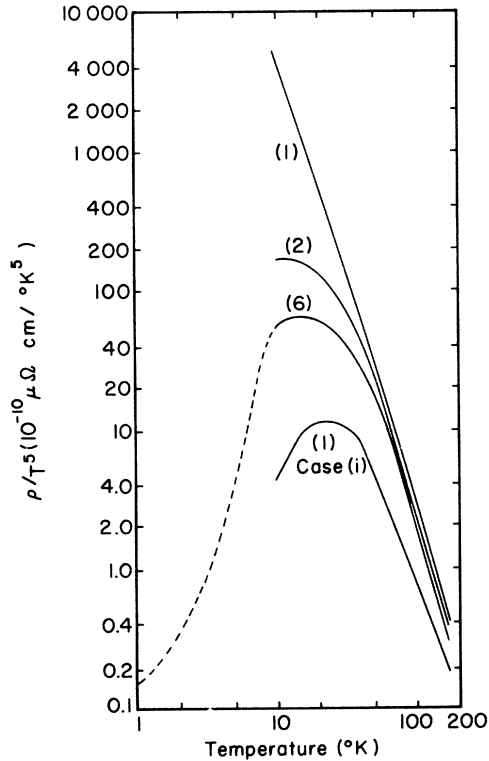


FIG. 13. Calculated resistivity divided by temperature to the fifth power vs temperature. The Fermi surface just touches the zone boundary. The quantity in brackets is the number of terms in the expansion of  $\phi(\hat{n})$ .

zone, with a radius equal to that of the free-electron Fermi sphere appropriate to aluminum.

Our results for the  $\cos\theta$  form of  $\phi(\hat{n})$  may be compared directly with the resistivities obtained by Dynes and Carbotte<sup>3</sup> in the temperature range from 40 to 100°K. These authors used a model identical to ours, and restricted themselves to the use of the  $\cos\theta$  form of  $\phi(\hat{n})$ . Their calculation differed from ours only in the technique used to evaluate the integrals; Dynes and Carbotte converted the integrals to three-dimensional form, while we have directly evaluated the four-dimensional integrals. At 40°K, the agreement between the two calculations is within 5%, but at 80°K, the resistivity we obtain is larger than that obtained by them by roughly 25%. There is evidence due to Hayman<sup>22</sup> that the procedure used by Dynes and Carbotte to fit the form factors could lead to the observed discrepancy between our result and theirs at 80°K.

It is not our intention to explore the high-temperature resistivity in detail. There are force constants available at 300°K which would be more appropriate than the 80°K force constants used here. Our one term value of 2.00  $\mu\Omega \text{ cm}$  for the resistivity at  $T = 300^\circ\text{K}$  is in good agreement with the value of 1.86  $\mu\Omega \text{ cm}$  quoted by Dynes and Carbotte for 300°K, so we feel our results are satisfactory at high temperatures. (Dynes and Carbotte also quote a value of 2.00  $\mu\Omega \text{ cm}$  at 300°K, but this result was obtained with force constants determined at 300°K.) At 300°K, the experimental value of the resistivity is 2.66  $\mu\Omega \text{ cm}$ . For aluminum, we find that for  $T \geq 100^\circ\text{K}$ , the calculated resistivity varies nearly linearly with temperature; the Debye temperature of aluminum is 390°K.

Our primary aim is to focus on the more interesting temperature range below 100°K. This is because Lawrence and Wilkins<sup>1</sup> have noted a considerable discrepancy between their very thorough calculations of the resistivity in this temperature region, and experimental values measured on very pure samples of aluminum. The discrepancy between their calculations and the data becomes less pronounced as the purity of the aluminum is reduced. They suggest that the origin of the discrepancy lies in the deviations of  $\phi(\hat{n})$  from the  $\cos\theta$  form, and that their calculations, which employ the  $\cos\theta$  form, are appropriate for the dirty limit where the form of  $\phi(\hat{n})$  is determined primarily by impurity scattering. In Fig. 14, the dashed curve represents the theoretical calculation of Lawrence and Wilkins, and the experimental results for clean and dirty samples as presented by Ekin and Bringer<sup>1</sup> are also displayed. The latter authors agreed, on the basis of their study of the effect of deviations of  $\phi(\hat{n})$  from the  $\cos\theta$  form in potassium, that in the clean limit the resistivity of Al should be

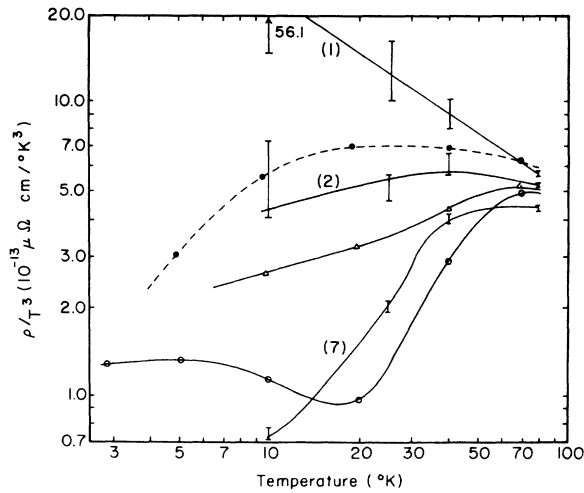


FIG. 14. Calculated resistivity divided by temperature to the third power vs temperature. The Fermi surface lies outside the first Brillouin zone. O, experimental data due to Ekin and Bringer (Ref. 1) for aluminum with a resistivity ratio of 7050.  $\Delta$ , experimental data due to Ekin and Bringer (Ref. 1) for aluminum with a resistivity ratio of 34.7.  $\bullet$ , the theoretical calculation of Lawrence and Wilkins (Ref. 1) for aluminum. The quantity in brackets is the number of terms in the expansion of  $\phi(\hat{n})$ .

greatly reduced from the values obtained through use of the  $\cos\theta$  form.

The results of our calculation for one, two, and seven terms in  $\phi(\hat{n})$  are shown in Fig. 14 as the solid lines. As we indicated in Sec. III, we experienced difficulty obtaining convergence at the lower temperatures, particularly when only a small number of terms were included in the expansion of  $\phi(\hat{n})$ , so the value of  $\phi(\hat{n})$  was considerable in the regions of the Fermi surface where the umklapp scattering is strong. The error bars in the figure are our estimate of the errors involved in the numerical calculations. The seven-term solution provides a remarkably good fit to the data to roughly 20°K, and we confirm with these calculations the suggestion of Lawrence and Wilkins that deviations from the  $\cos\theta$  form of  $\phi(\hat{n})$  are responsible for the discrepancy between theory and experiment discussed earlier. At 20°K, the lattice resistivity is roughly  $8 \times 10^{-4} \mu\Omega \text{ cm}$ , and the residual resistivity is  $4 \times 10^{-4} \mu\Omega \text{ cm}$ . Thus, we expect the results of our calculation, where  $\phi(\hat{n})$  is determined in the presence of only electron-phonon scattering, to begin to deviate from the experimental data at temperatures in the vicinity of 20°K.

Since Fig. 14 provides a clear description of the data and the calculations, we do not present a plot of  $\rho/T^5$ . However, if this is done, even at temperatures as low as 10°K, we see no sign of the onset of the freezing out of the umklapp processes

which in both case (i) and case (ii) causes the maximum and subsequent decrease in the values of  $\rho/T^5$  as the temperature is lowered, although for case (iii), we have reached a plateau in the plot of  $\rho/T^5$  by the time  $T = 10^\circ\text{K}$  for the nine term expansion of  $\phi(\hat{n})$ . Note that the apparent  $T^3$  term seen in the resistivity of aluminum (see the data in Fig. 14, where  $\rho/T^3$  becomes constant below about 10°K) occurs in the data before the umklapp processes are frozen out, so this term in aluminum may possibly be explained by a calculation which allows the form of  $\phi(\hat{n})$  to be affected by impurity scattering through the temperature region where the umklapp processes are freezing out. It is important in this regard to note that the  $T^3$  variation of the resistivity reported in copper (see, for example, the recent work of Rumbold<sup>19</sup>) is seen very clearly at temperatures well below the point where the umklapp processes have frozen out, and where the lattice resistivity is a small fraction of the total.

In the case of aluminum, it would be very interesting to compute the temperature dependence of the resistivity for a model which allows the form of  $\phi(\hat{n})$  to be influenced by the presence of impurity scattering. Quite clearly, this will increase the lattice contribution to the resistivity, and the question of whether this will raise the value of the lattice resistivity sufficiently to account for the observed behavior of the resistivity is an intriguing one.

## V. FINAL REMARKS

The calculations presented in Sec. III and IV demonstrate the importance of utilizing the proper form of  $\phi(\hat{n})$  in the computation of the electrical resistivity, particularly as the temperature is lowered, and "hot spots" where umklapp scattering is strong develop on the Fermi surface. In fact, for case (ii), where the Fermi surface touches the zone boundary, it is important to use the full form of  $\phi(\hat{n})$  at all temperatures.

The use of the correct form of  $\phi(\hat{n})$  in the calculation of the electrical resistivity allows us to obtain rather good agreement between our calculated resistivities and experimental data, even though we use an oversimplified description of the Fermi surface. At high temperatures, one is perhaps not surprised to see this, simply because the scattering rate is not highly anisotropic, and large deviations from free electron character [say in case (i)] occur only over a relatively small fraction of the total solid angle in the integrations. However, as the temperature is lowered, umklapp scattering near those portions of the Fermi surface which lie close to the zone boundary causes these regions, where the use of a model with a spherical Fermi surface is clearly a poor approximation, to make a large contribution to the variational expres-

sion for  $\rho$ , if the  $\cos\theta$  form of  $\phi(\hat{n})$  is used in the calculation. However, as we have seen, if one uses a more accurate form for  $\phi(\hat{n})$  in the calculation, this function develops pronounced dimples precisely where the umklapp scattering is strong. This suppresses the contributions from these portions of the Fermi surface to the resistivity, and enhances contributions from those portions of the Fermi surface which lie farther from the zone boundary, and which are described by the spherical Fermi surface model in a reasonable way. We have demonstrated this point by the series of calculations which compare, for case (i) and case (ii), the resistivities calculated for the model with the full spherical Fermi surface, and those calculated with the  $14^\circ$  caps removed; one sees that the values obtained for the resistivity are quite close for these two cases, as long as the full seven- or nine-term expression for  $\phi(\hat{n})$  is used.

In all the cases we have examined, the calculation of the ideal electrical resistivity breaks down at low temperatures. To perform an accurate calculation of the electrical resistivity at temperatures below  $10^\circ\text{K}$  in all cases would require more terms in the expansion of  $\phi(\hat{n})$ . At the same time, considerably finer meshes would be required in the integration schemes. Once the convergence becomes poor, it deteriorates very rapidly as the temperature is lowered further, and it is a non-trivial matter to perform reliable calculations well below  $10^\circ\text{K}$ . Physically, this problem occurs because as the temperature is lowered, the "hot spots" on the Fermi surface subtend a smaller and smaller solid angle as the umklapps freeze out. One needs a progressively finer mesh to compute the integrations accurately. Also, the dimples in  $\phi(\hat{n})$  presumably will sharpen up, so many more terms in the cubic harmonics are required to describe them accurately. When one enters this temperature regime, it would most likely be best not to try to extend our approach in a brute force manner, but rather to develop a scheme more suited to dealing with the behavior expected in the low-temperature limit, i. e., one might use for  $\phi(\hat{n})$  not the cubic harmonic expansion but an analytic form (with variational parameters) which mimics the expected behavior.

We have not pursued this question of the accurate computation of the electrical resistivity at low temperatures for our model, primarily because one encounters a new set of problems in addition to those just described, if one wishes to make contact with the existing data. When  $T \leq 10^\circ\text{K}$ , in the samples studied experimentally, the lattice resistivity and the contribution  $\rho_0$  from impurity scattering become comparable in magnitude. Then the form of  $\phi(\hat{n})$  must be determined by a scheme which simultaneously includes impurity and electron-

phonon scattering. One expects the impurity scattering to modify strongly the form of  $\phi(\hat{n})$  when  $\rho_0$  and the lattice resistivity are comparable. When the Fermi surface in the model does not touch the zone boundary, presumably  $\phi(\hat{n})$  will be driven toward the  $\cos\theta$  form. If we were to carry out such a calculation for our model, it would be questionable if we could compare the results to experimental data on real fcc metals. This is because when  $\phi(\hat{n})$  has the  $\cos\theta$  form, we know the lattice contribution to the resistivity becomes quite sensitive to the properties of the model Fermi surface near the zone boundaries. This is clearly demonstrated by our calculations of  $\rho$  with the  $14^\circ$  caps removed, where we found  $\rho$  changed dramatically when the caps were removed at low temperatures, when the  $\cos\theta$  form of  $\phi(\hat{n})$  is used in the calculation.

To summarize briefly these rather lengthy comments: in each case we have examined, we find our calculation scheme breaks down by the time the temperature reaches  $\approx 10^\circ\text{K}$ , although the results appear quite satisfactory to us at higher temperatures. To improve the calculations below  $10^\circ\text{K}$  would likely involve extensive revisions of the computation scheme and, if we wish to make contact with data, will also require the use of a much more realistic model. This latter conclusion is not a new one, of course. It is clear from Ehrlich's work<sup>5</sup> and the more recent discussions in the paper by Lawrence and Wilkins<sup>1</sup> that at low temperatures, the temperature dependence of the lattice resistivity is quite sensitive to a proper description of the Fermi surface. We refer the reader to the discussion of the  $T^2$  term in the paper by Lawrence and Wilkins.

We do feel progress can be made by a more detailed study of the temperature dependent portion of the electrical resistivity of copper based alloys. This is an area we are currently exploring.

#### APPENDIX A: CONVERGENCE OF CALCULATIONS

Throughout the entire study we encountered considerable difficulty in obtaining convergence of the results, particularly in case (ii). The purpose of this appendix is to indicate the sort of convergence we obtained for this case, in which the Fermi surface touches the zone boundary.

In Table XII the effect of mesh on the resistivity is presented. In the high-temperature region the convergence is to better than 1% except for the one term solution. The convergence difficulty is, in fact, quite pronounced for the one term solution down to  $10^\circ\text{K}$ . The problem arises here from the singularity in the integrals that exists for scattering from the point where the surface touches the zone boundary to points near the opposite pole. A more refined mesh in the area would affect additional

TABLE XII. Convergence of resistivity ( $\mu\Omega$  cm) for the case where the Fermi surface just touches the zone boundary.

Temp. (°K)	Multiply table value by	Number of terms in the expansion of $\phi(\hat{n})$									Mesh size
		1	2	3	4	5	6	7	8	9	
298	$10^0$	7.35	6.53	6.53	5.43	5.32	5.15	5.15	5.13	5.13	<i>A</i>
	$10^0$	7.19	6.49	6.49	5.46	5.32	5.15	5.15	5.15	5.15	<i>B</i>
	$10^0$	6.84	6.41	6.41	5.49	5.38	5.23	5.18	5.18	5.18	<i>C</i>
49	$10^{-1}$	5.61	3.76	3.76	2.57	2.46	2.29	2.28	2.28	2.28	<i>B</i>
	$10^{-1}$	5.15	3.92	3.92	2.64	2.51	2.35	2.35	2.31	2.30	<i>C</i>
20	$10^{-2}$	11.7	1.48	1.34	0.943	0.909	0.877	0.758	0.662	0.625	<i>B</i>
	$10^{-2}$	9.71	2.27	2.24	1.23	1.12	1.06	0.925	0.699	0.649	<i>C</i>
10	$10^{-4}$	363.0	5.71	2.01	1.88	0.537	0.535	0.493	0.448	0.435	<i>B</i>
	$10^{-4}$	258.0	8.06	4.05	3.46	2.82	2.82	2.62	1.57	1.25	<i>C</i>
	$10^{-4}$	279.0	8.16	4.01	3.46	2.73	2.73	2.58	1.58	1.32	<i>D</i>

changes  $\lesssim 10\%$  at 298 °K and  $\lesssim 50\%$  at 10 °K. This difficulty primarily arises when the  $\cos\theta$  form of  $\phi(\hat{n})$  is used, and becomes much less severe as  $\phi(\hat{n})$  is allowed to decrease near the (1, 1, 1) point of the zone. Since from general considerations we know the full form of  $\phi(\hat{n})$  must vanish at the (1,1,1) point for case (ii), we have not pursued the convergence question further.

Convergence in the resistivity when the more complete forms of  $\phi(\hat{n})$  are used has occurred to within  $\approx 5\%$  for the *C* to *D* transition at 10 °K, which suggests that our usage of the *C* mesh is appropriate for 20 and 30 °K. When one goes from the *B* to the *C* mesh at 49 °K, the resistivity changes by only  $\approx 5\%$ , so that it seems appropriate to use the *B* mesh above 49 °K. At  $T \geq 298$  °K the *A* mesh seems to be appropriate since it differs by  $\approx 1\%$  from the *C* mesh.

Next consider the results for the expansion coefficients presented in Table XIII. For the moment ignore the 10 °K data. Note that there is considerable variation in the third coefficient. Consulting

Table V in the main text we see this is a plausible variation because the addition of the third term has little effect on the resistivity, and presumably also on  $\phi(\hat{n})$ .

Upon considering the remaining coefficients above 10 °K, we see changes  $\lesssim 25\%$  at 298 °K give some measure of their accuracy at that temperature. By 49 °K the *B* mesh seems more effective for getting at the fourth and sixth coefficients, but the second coefficient is off by  $\approx 50\%$  if it is used in the calculation.

For  $T \leq 49$  °K we expect the *C* mesh has given the second, third, and fifth coefficients to  $\lesssim 5\%$  based on the *C* to *D* changes in the 10 °K results. There is some uncertainty as to how closely the sixth term has converged.

Finally, consider the results at 10 °K. Here we see that the sixth term has reached a value which is not changing but oscillates quite markedly in going there. Note also that the third coefficient has altered quite drastically from its values at higher temperatures, perhaps reflecting the fact

TABLE XIII. Convergence of the normalized expansion coefficients when the Fermi surface just touches the zone boundary.

Temp. (°K)	Index of the coefficient						Mesh size
	1	2	3	4	5	6	
298	$10^0$	$10^{-1}$	$10^{-2}$	$10^{-2}$	$10^{-1}$	$10^{-4}$	<i>B</i>
	1.00	1.65	-1.44	1.20	-2.40	2.20	<i>B</i>
49	1.00	1.26	-5.40	1.22	-2.65	2.04	<i>C</i>
	1.00	1.35	-19.2	1.58	-2.71	3.31	<i>B</i>
30	1.00	0.744	-25.6	1.67	-3.28	3.41	<i>C</i>
	1.00	1.66	-24.3	1.63	-2.74	3.34	<i>B</i>
20	1.00	0.550	-36.7	1.80	-3.25	3.80	<i>C</i>
	1.00	4.34	+9.65	1.38	-1.45	2.11	<i>B</i>
10	1.00	1.57	-20.0	1.73	-2.81	3.01	<i>C</i>
	1.00	1.64	133.0	0.189	6.85	-19.4	<i>B</i>
	1.00	1.26	103.0	0.592	4.07	0.051	<i>C</i>
	1.00	1.30	105.0	0.554	4.26	0.025	<i>D</i>

that at 10°K it does alter the resistivity of Table V, but seems to have converged.

Considerations such as the above have led us to the accuracies quoted for  $\rho$  and  $\eta_i$  in the text. In addition, the comparison of our results for alumi-

num with those of Dynes and Carbotte<sup>3</sup> and a variety of tests not cited here involving cruder meshes, and also with the  $z$  axis of the Fermi sphere rotated off parallelism with the field, all support the results we have presented.

\*Research sponsored by the Air Force Office of Scientific Research, Office of Aerospace Research, USAF, under Grant No. AFOSR 70-1936.

†Permanent address: Dept. of Physics, Brock University, St. Catharines, Ontario, Canada.

<sup>1</sup>J. W. Ekin and A. Bringer, Phys. Rev. B (to be published); M. P. Greene and W. Kohn, Phys. Rev. **137**, 513 (1965); Yu Kagan and A. P. Zhernov, Zh. Eksp. Teor. Fiz. **xx**, (19xx) [Sov. Phys.-JETP **33**, 990 (1971)]; W. E. Lawrence and J. W. Wilkins, Phys. Rev. B **6**, 4466 (1972).

<sup>2</sup>J. M. Ziman, *Electrons and Phonons*, (Oxford U. P., Oxford, England, 1960), Chap. 9.

<sup>3</sup>R. C. Dynes and J. P. Carbotte, Phys. Rev. **175**, 913 (1968).

<sup>4</sup>S. K. Srivastava, Nuovo Cimento Lett. **6**, 353 (1973).

<sup>5</sup>P. G. Klemens and J. L. Jackson, Physica (Utr.) **30**, 2031 (1964); A. Ehrlich, Phys. Rev. B **1**, 4537 (1970).

<sup>6</sup>R. Peierls, Ann. Phys. (Leipzig.) **12**, 154 (1932).

<sup>7</sup>J. A. Moriarty, Phys. Rev. B **1**, 1363 (1970).

<sup>8</sup>R. M. Nicklow, G. Gilat, H. G. Smith, L. J. Raubheimer, and M. K. Wilkinson, Phys. Rev. **164**, 962 (1967).

<sup>9</sup>E. C. Svensson, B. N. Brockhouse, and J. M. Rowe, Phys. Rev. **155**, 619 (1967).

<sup>10</sup>We have studied the effect on  $\phi(\hat{n})$  of including seven through nine terms, and we find no qualitative change

of significance.

<sup>11</sup>W. A. Harrison, *Pseudopotentials in the Theory of Metals* (Benjamin, New York, 1966).

<sup>12</sup>G. Gilat and R. M. Nicklow, Phys. Rev. **143**, 487 (1966).

<sup>13</sup>NBS Technical Note No. 365, *Survey of Electrical Resistivity Measurements on 16 Pure Metals in the Temperature Range 0°K to 273°K*, U. S. Department of Commerce, Natl. Bur. Stds. (U. S. GPO, Washington, D. C., 1968).

<sup>14</sup>N. E. Cussak, Rept. Prog. Phys. **26**, 361 (1963).

<sup>15</sup>W. V. Houston, Rev. Mod. Phys. **20**, 161 (1968).

<sup>16</sup>K. Krebs, Phys. Lett. **10**, 12 (1964).

<sup>17</sup>J. T. Schriempf, Proceedings of the Seventh Conference on Thermal Conductivity, NBS Grasthersburg, 1967, NBS Special Publication **302**, 249 (1968).

<sup>18</sup>G. K. White and S. B. Woods, Philos. Trans. R. Soc. Lond. A **251**, 273 (1959).

<sup>19</sup>E. R. Rumbo, J. Phys. F **3**, L9 (1973).

<sup>20</sup>I. A. Campbell, A. D. Caplin, and C. Rizzuto, Phys. Rev. Lett. **26**, 239 (1971).

<sup>21</sup>R. S. Crisp, W. G. Henry, and P. A. Schroeder, Philos. Mag. **10**, 533 (1964).

<sup>22</sup>B. Hayman (private communication). He used the same computer program as Dynes and Carbotte (Ref. 3), but a different method of fitting the form factors and obtained  $\rho = 0.28 \mu\Omega \text{ cm}$  at 80°K.